



## Influence of Black Shale Composition on Methane Adsorption and Gas Content: Implications For Gas Storage in the Longmaxi Black Shal

Haihua Zhu<sup>1,2,3\*</sup>, Tingshan Zhang<sup>1,2</sup>, Jun Lang<sup>1,2</sup>, Jianli Zeng<sup>1,2</sup>, Xing Liang<sup>4</sup>, Yong He<sup>4</sup>, Gaocheng Wang<sup>4</sup>, Junjun Li<sup>4</sup>

<sup>1</sup> State Key Laboratory of Oil and Gas Reservoir Geology and Exploitation, Chengdu, China

<sup>2</sup> School of Geoscience and Technology, Southwest Petroleum University, Chengdu, China

<sup>3</sup> Unconventional oil and gas Assessment Center, Southwest Petroleum University, Chengdu, China

<sup>4</sup> PetroChina, Zhejiang Oil Field Company, Hangzhou, China

\*Email of Corresponding Author: zhhswp@163.com

### ABSTRACT

The influence of shale composition on methane adsorption capability and gas content is investigated using 14 samples from Well YS8 in the southern Sichuan Basin, China. The results show that the Langmuir adsorption capacity of the Longmaxi shale is mainly a function of the total organic carbon (TOC) content. When TOC is ~1.1%, 50% CH<sub>4</sub> is adsorbed onto the surface of the organic matter. The mineral content has limited control on the adsorption capacity of the Longmaxi shales. Organic matter is also a major control on gas content when TOC content is <1.0%. When TOC is >1.0%, gas content remains constant, indicating that gas preservation is more important than gas generation and rock adsorption capacity. Scatter plots of TOC versus gas content and, Langmuir adsorption capacity shows that when TOC is <2.0%, CH<sub>4</sub> occurs both as free and adsorbed gas, and CH<sub>4</sub> occurs mainly as adsorbed gas when TOC is >2.0%.

*Keywords:* Shale; Methane; Adsorption; TOC; Sichuan.

## Influencia de la composición de lutitas negras en la absorción de metano y el contenido de gas: implicaciones para el almacenamiento de las lutitas negras de Longmaxi

### RESUMEN

La influencia de la composición de lutitas en la capacidad de absorción del metano y el contenido de gas se analiza en este trabajo a partir de 14 muestras del pozo YS8 en la cuenca de Sichuan, al suroeste de China. Los resultados muestran que la capacidad de absorción Langmuir para las lutitas de Longmaxi es principalmente una función del contenido de Carbono Orgánico Total (TOC, del inglés Total Organic Carbon). Cuando el índice TOC es ~1.1%, el 50 % del CH<sub>4</sub> (capacidad máxima de absorción de la función Langmuir) es absorbido por la superficie de materia orgánica. El contenido mineral tiene un control limitado en la capacidad de absorción de las lutitas de Longmaxi. La materia orgánica también tiene un control mayor en el contenido de gas cuando el índice TOC es <1.0 %. Cuando el TOC es >1.0 %, el contenido del gas es constante, lo que indica que la preservación del gas es más importante que la generación del gas, y la capacidad de absorción de la roca. Diagramas de dispersión del TOC frente al contenido de Gas y de la capacidad de absorción Langmuir muestran que el TOC es <2.0 %, que el CH<sub>4</sub> se alcanza tanto en gas libre como en gas absorbido y que este ocurre principalmente cuando el gas absorbido tiene un nivel TOC de >2.0 %.

*Palabras clave:* lutitas; metano; adsorción, Carbono Orgánico Total.

### Record

Manuscript received: 14/11/2017

Accepted for publication: 21/03/2017

### How to cite item

Pages 59-63

DOI: <http://dx.doi.org/10.15446/esrj.v22n1.70539>

## 1. Introduction

The Wufeng–Longmaxi black shale in the Sichuan Basin is the first shale gas reservoir to be commercially produced in China. By 2016, four national demonstration areas of marine shale gas production (the Weiyuan, Changning, Zhaotong, and Jiaoshiba shale gas plays) had been established in Sichuan, Chongqing, and Yunnan. However, the heterogeneity of black shales concerning the total organic carbon (TOC) content and mineral composition, which control gas generation and reservoir quality, limits the predictability of the shale gas ‘sweet spot’ (Chen et al., 2015; Farrooqi et al., 2017). Therefore, it is necessary to evaluate the control of shale composition on storage capability and shale gas content.

In this study, 14 samples from Well YS8 in the southern Sichuan Basin are analyzed to investigate the geochemistry, petrology, and methane adsorption capacity of the shale by TOC testing, XRD analysis, and methane adsorption experiments. By discussing the relationship between shale composition and methane adsorption capacity, and shale gas content, we hope to identify the main factors that influence the storage capability and gas content of shale reservoirs, which can then be applied to other shale reservoirs with a similar preservation condition to that of the Longmaxi shale.

## 2. Geological setting

The study area is located in the Changning shale gas field in the southern Sichuan Basin (Figure 1). The Sichuan Basin is located on the northwestern Yangtze Plate and is the remnant of the lower Paleozoic Upper Yangtze cratonic basin (Lu et al., 2006; Karami et al., 2017). The Wufeng–Longmaxi formations were formed in a continental shelf sea (Zhang et al., 2012; Liang et al., 2016) during the Late Ordovician and early Silurian (Su et al., 2009; Sunny et al., 2018). The thickness of the strata varies from several meters to >300 m, with depocenters located in the southern and eastern parts of the basin (Guo et al., 2014; Nwankwo and Nkwankwoala, 2018). The Wufeng–Longmaxi shale is now mainly thermally over-mature (Liang et al., 2011).

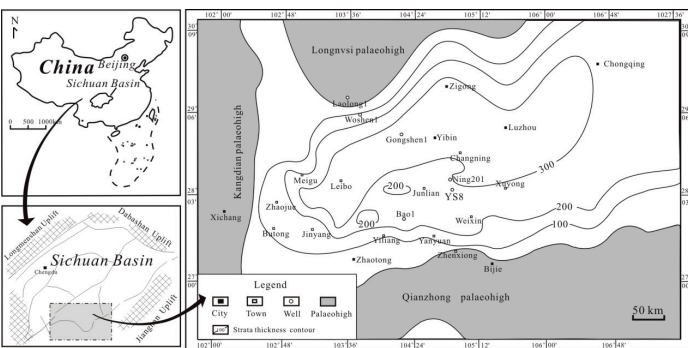


**Figure 1.** Study area and paleogeography of the Wufeng and Longmaxi formations

## 3. Samples and methods

Fourteen shale core samples with burial depths ranging from 2382.43 to 2512.42 m were selected for analysis from shale gas well YS8 in the study area. The whole-rock mineral compositions were determined by XRD analysis. The samples were crushed to powder, and XRD analyses were performed using an X'Pert Pro X-ray diffractometer with a Cu anode at 40 kV, 20 mA, and 0.154 nm wavelength. The TOC was measured with a LECO CS-400 carbon–sulfur analyzer (combustion at temperatures of >800°C). Before analysis, carbonate from the samples was removed using hydrochloric acid (1:1).

The methane adsorption capacity was investigated using a PCTProE&E high-pressure adsorption–desorption instrument. The samples were dried for 48 h at 110°C and tested in a sample cell with a temperature of

30°C (±0.2°C) and a pressure of 0–11 MPa. The room temperature was 30°C and humidity was 1%–2%. The methane adsorption capacity was calculated in m<sup>3</sup>/t (STP: 0°C, 101.325 kPa) using the material balance principle and the volumetric method (Krooss et al., 2002; Ali et al., 2018).

The shale gas content of core samples comprises the desorbed gas, residual gas, and lost gas. Desorbed gas and residual gas were measured using canister desorption of the fresh cores. The lost gas was calculated using USBM methods.

## 4. Results

### 4.1 Gas content

The gas content of the 14 samples ranges from 1.49 to 3.43 m<sup>3</sup>/t with an average of 2.59 m<sup>3</sup>/t. Gas content varies with depth (Table 1), showing a decreasing upward trend. The shale samples with a gas content of >2.0 m<sup>3</sup>/t are found mainly between 2486.77 and 2512.42 m depth.

### 4.2 TOC content

The TOC content of the 14 samples ranges from 0.34% to 4.72% with an average of 1.81%. The maximum TOC (>2.0%) was obtained for six shale samples with a burial depth between 2491.48 and 2512.15 m (Table 1). The samples from depths of <2481 m have TOC contents of <1.0%. A similar upward decreasing trend in the TOC content of shale has been reported elsewhere in the Upper Yangtze region (e.g., Liang et al., 2011; Guo et al., 2014; Asghar et al., 2018).

**Table 1.** TOC, Gas content, and Langmuir adsorption capacity of the Longmaxi shales in YS8

Sample	Depth (m)	TOC%	Gas content m <sup>3</sup> /t	Langmuir adsorption capacity m <sup>3</sup> /t
YS8-1	2382.43	0.34	1.49	1.01
YS8-2	2386.75	0.64	1.97	1.23
YS8-3	2391.22	0.42	1.84	0.95
YS8-4	2467.47	0.77	2.96	1.48
YS8-5	2471.28	0.62	2.31	1.2
YS8-6	2475.11	0.76	2.28	1.37
YS8-7	2481.09	1.00	2.27	1.77
YS8-8	2486.77	1.53	3.36	2.55
YS8-9	2491.48	2.21	2.92	3.16
YS8-10	2496.19	3.89	2.55	4.11
YS8-11	2501.61	3.20	3.43	3.76
YS8-12	2506.17	2.56	2.86	3.03
YS8-13	2510.38	2.61	2.93	3.43
YS8-14	2512.15	4.72	3.11	3.99

### 4.3 Mineral composition

The XRD data show that the 14 black shale samples from well YS8 are dominated by carbonate, clay minerals, and quartz, with subordinate feldspar and pyrite (Table 2).

The carbonate mineral content ranges from 15.6% to 62.0% (average 32.2%), the clay mineral content ranges from 14.1% to 37.2% (average 28.1%), and the quartz content ranges from 15.3% to 41.7% (average 28.3%). The feldspar content ranges from 4.2% to 16.4% (average 8.0%) and the pyrite content from 1.5% to 9.2% (average 3.4%).

Mineral composition data show vertical variations. The three samples (YS8-1 to YS8-3) with the minimum burial depths are characterized by high carbonate and quartz contents, moderate clay mineral contents, and low TOC contents (Hasan, 2018). The four deepest samples (YS8-11–YS8-14) contain high carbonate and TOC contents, and low clay contents. These seven middle samples (YS8-4 to YS8-10) contain low carbonate, high clay, and moderate TOC contents.

**Table 2.** Mineral compositions of Longmaxi shale samples from well YS8

samples	depth (m)	quartz	K-feldspar	plagioclase	calcite	dolomite	pyrite	clay
YS8-1	2382.43	20.9	1.3	4.4	37.7	7.4	1.5	26.8
YS8-2	2386.75	21.0	0.9	4.4	31.4	6.5	1.9	33.9
YS8-3	2391.22	25.7	1.1	3.8	29.5	8.4	2.2	29.3
YS8-4	2467.47	35.0	2.6	9.7	10.6	5.0	2.8	34.3
YS8-5	2471.28	27.5	3.5	12.9	14.6	7.9	2.4	31.2
YS8-6	2475.11	32.7	5.4	11.0	14.2	5.9	2.3	28.5
YS8-7	2481.09	31.4	2.2	8.4	11.6	7.5	3.2	35.7
YS8-8	2486.77	33.5	1.6	5.7	11.8	5.9	4.3	37.2
YS8-9	2491.48	26.9	1.1	5.6	15.6	7.8	9.2	33.8
YS8-10	2496.19	41.7	1.4	5.2	9.0	8.3	4.8	29.6
YS8-11	2501.61	27.4	1.2	4.5	15.3	27.0	4.9	19.7
YS8-12	2506.17	32.8	1.1	3.5	25.8	19.3	3.4	14.1
YS8-13	2510.38	15.3	0.6	3.6	44.1	17.9	2.7	15.8
YS8-14	2512.15	24.1	0.9	4.1	31.3	13.4	2.6	23.6

**4.4 Methane adsorption**

Methane adsorption isotherms are shown in Figure 2. The measured isotherms at different temperatures can be fitted well to the Langmuir function. The Langmuir maximum CH<sub>4</sub> adsorption capacities range from 0.95 to 4.11 m<sup>3</sup>/t, with higher capabilities found for samples YS8-9 to YS8-14 (>3.1 m<sup>3</sup>/t). The adsorption capacities of samples YS8-1 to YS8-7 are <1.8 m<sup>3</sup>/t.

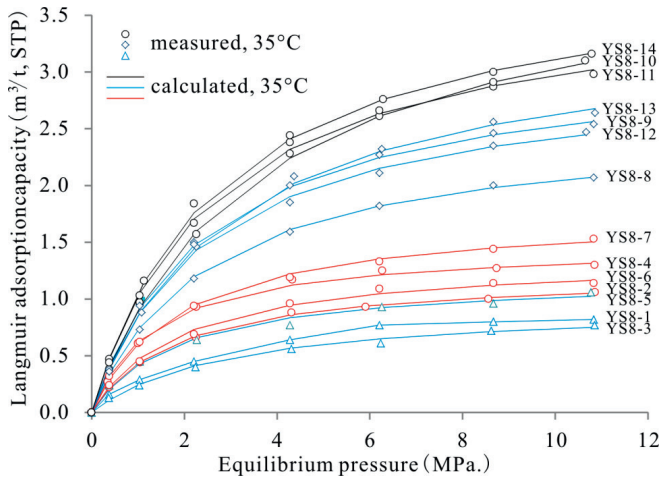


**Figure 2.** Methane adsorption isotherms of the studied samples

**5 Discussion**

**5.1 Controls on CH<sub>4</sub> adsorption in black shales**

Figure 3 shows scatter plots of the Langmuir maximum CH<sub>4</sub> adsorption (Γ<sub>L</sub>) versus shale composition (organic matter and minerals). Γ<sub>L</sub> shows a strong positive correlation with TOC.

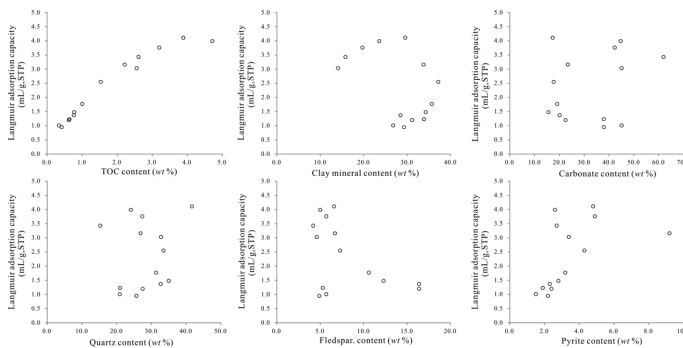


**Figure 3.** Langmuir adsorption capacity versus shale composition

Equation (1) shows the result of linear regression between Γ<sub>L</sub> and TOC content, based on the experimental measurements of this study.

$$\Gamma_L = 0.8137 \times \text{TOC} + 0.891 \quad (1)$$

Where Γ<sub>L</sub> is in units of m<sup>3</sup>(CH<sub>4</sub>)/t rock and TOC is the total organic carbon content in units of wt%. The regression provides an empirical basis for estimating the Langmuir maximum CH<sub>4</sub> adsorption capacity from TOC content in a shale reservoir. A similar correlation between gas sorption capacity and TOC content at 30°C and 6 MPa pressure has been observed in previous studies (Chalmers and Bustin, 2007a,b; Ross and Bustin, 2007, 2009; Zhang et al., 2012; Msarah and Alsier, 2018).

The strong correlation between Γ<sub>L</sub> and TOC content is due to the massive surface area of organic matter for CH<sub>4</sub> adsorption. Cao et al. (2015) reported that kerogen of the Longmaxi shale in the Sichuan Basin has a surface area of ~161.2 m<sup>2</sup>/g, which is much higher than that of quartz and carbonate minerals.

The proportion of CH<sub>4</sub> adsorbed onto organic matter can be estimated by Equation (2).

$$\Gamma_L = \text{TOC} \times \Gamma_{\text{org}} + \text{Mineral content} \times \Gamma_{\text{rock}} \quad (2)$$

Where Γ<sub>org</sub> is the Langmuir CH<sub>4</sub> adsorbed onto organic matter and Γ<sub>rock</sub> is the Langmuir CH<sub>4</sub> adsorbed onto minerals. Mineral content is the total mineral content in wt%, TOC is the total organic carbon content in wt%, and Mineral content + TOC = 100%.

In the model, we assume that i) CH<sub>4</sub> is adsorbed onto two types of solid material (organic matter and minerals), and ii) Γ<sub>rock</sub> remains constant, and the change of Γ<sub>rock</sub> due to the variations in type and relative content of minerals is negligible compared with the influence of TOC content.

Based on Equation (2), when TOC is 0% all the CH<sub>4</sub> is adsorbed onto inorganic mineral surfaces, with 0.891 m<sup>3</sup> of CH<sub>4</sub> adsorbed for every ton of inorganic minerals. As TOC content increases and mineral content decreases, the proportion of CH<sub>4</sub> adsorbed onto organic matter increases, and when TOC is ~1.05%, ~50% of the CH<sub>4</sub> is adsorbed onto the surface of organic matter (Figure 4).

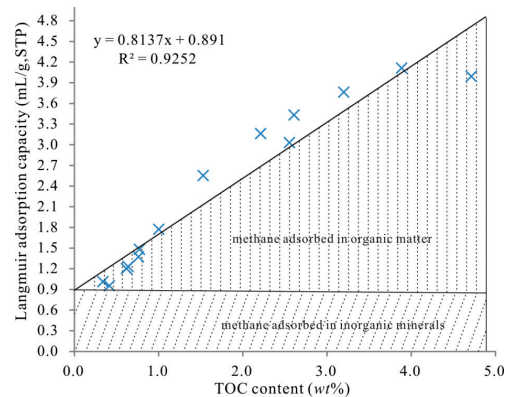


**Figure 4.** Relative proportion of CH<sub>4</sub> adsorbed on organic matter and minerals

**5.2 Methane absorption capacity and shale gas content**

Due to the high-to-over thermal maturity of organic matter and strong tectonic deformation, the gas content of the Longmaxi shales is controlled by many factors, especially the preservation condition, natural matter abundance, and reservoir quality (e.g., Zou et al., 2010; Rahim et al., 2018).

In the shale samples from Well YS8, the preservation conditions and thermal evolution processes of organic matter are similar, thus enabling an evaluation of the influence of shale composition on shale gas content.

Scatter plots of gas content versus shale composition are shown in Figure 5. Poor relations are found between gas content versus mineral composition. Regular change of shale gas content with TOC content is observed. As TOC content increases, gas content first increases and then remains constant. This relationship indicates that organic matter is a significant control on gas content when TOC content is <2.0%. When TOC is >2.0%, the adsorption surface area is sufficient, and other factors such as gas preservation condition may influence the amount of residue gas (Indan et al., 2018). A similar pattern is obtained when gas content is plotted against pyrite content. Pyrite content is considered an indicator of redox conditions and is usually found in larger concentrations when TOC content is high, which may explain this similar correlation of gas content versus pyrite and TOC contents.

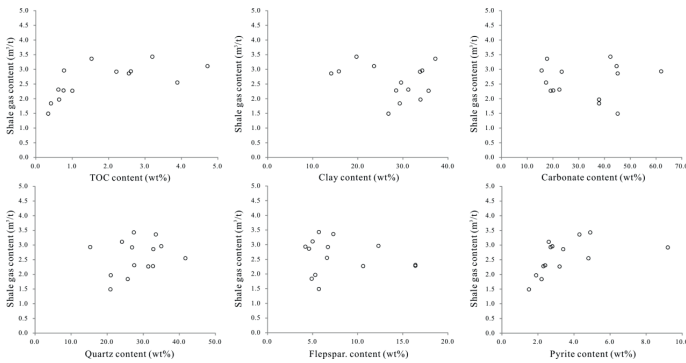


Figure 5. Shale gas content versus shale composition

The scatter plots of TOC content versus gas content, and Langmuir adsorption capacity shows that when TOC is <2.0% the gas contents are higher than the Langmuir adsorption capacity of shale (Figure 6). Therefore, CH<sub>4</sub> partially occurs as free gas within the macropores of the shale (Nwankwoala and Oborie, 2018; Nwankwoala and Ememu, 2018). When TOC is >2.0%, the gas contents are less than the Langmuir adsorption capacity of shale, indicating that CH<sub>4</sub> tends to occur mainly as adsorbed gas, as the surface area of organic matter is sufficient for gas absorption.

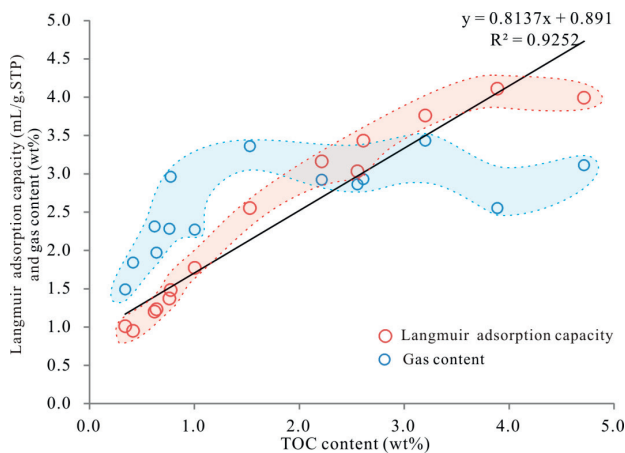


Figure 6. The Scatter plots of TOC content versus gas content and Langmuir adsorption capacity

## 6. Conclusions

The Langmuir adsorption capacity of the Longmaxi shale is mainly a function of TOC content. The regression shows that when TOC content is ~1.1%, 50% of the CH<sub>4</sub> is adsorbed onto the organic matter. The mineral content has control on the adsorption capacity of the Longmaxi shales. Organic matter is a major control on gas content when TOC content is <2.0%.

When TOC is >2.0%, gas content remains constant and is a function of organic matter. Scatter plots of gas content and Langmuir adsorption capacity versus TOC content show that when TOC is <2.0%, CH<sub>4</sub> occurs as both free and adsorbed gas and that CH<sub>4</sub> occurs mainly as adsorbed gas when TOC is >2.0%.

## 7. Acknowledgments

This work was funded by the Young Scholars Development Fund of Southwest Petroleum University (SWPU) (201499010046), China postdoctoral science foundation (2015M580797), National Natural Science Foundation of China (41772150) and National Science and Technology Major Project (2017ZX05063002-009).

## References

- Ali, W., Nasir, M. S., Nasir, A., Rashid, H., Ayub, I., Gillani, S. H., & Latif, M. J. (2018). Assessment of Carbon Footprints in Terms of CO<sub>2</sub> Of Diesel Generator, Pakistan. *Earth Sciences Pakistan*, 2(1), 15-17.
- Asghar, Z., Ali, W., & Nasir, A. (2018). Atmospheric Monitoring for Ambient Air Quality Parameters and Source Apportionment of City Faisalabad, Pakistan. *Earth Sciences Pakistan*, 2(1), 01-04.
- Cao, T. T., Song, Z. G., & Wang, S. B. (2015). A comparative study of the specific surface area and pore structure of different shales and their kerogens. *Science China Earth Sciences*, 58(4), 510-522.
- Chalmers, G. R. L., & Bustin, R.M. (2007). The organic matter distribution and methane capacity of the Lower Cretaceous strata of northeastern British Columbia, Canada. *International Journal of Coal Geology*, 70, 223-239.
- Chen, L., Lu, Y., & Jiang, S. (2015). Heterogeneity of the Lower Silurian Longmaxi marine shale in the southeast Sichuan Basin of China. *Marine and Petroleum Geology*, 65, 232-246.
- Farooqi, Z. U. R., Nasir, M. S., & Nasir, A. (2017). Evaluation and analysis of traffic noise in different zones of Faisalabad an industrial city of Pakistan. *Geology, Ecology, and Landscapes*, 1(4), 232-240.
- Guo, T. L., & Zhang, H. R. (2014). Formation and enrichment mode of Jiaoshiba shale gasfield, Sichuan Basin. *Petroleum. Exploration & Development*, 41, 31-40.
- Hasan, M. (2018). Effect of Rhizobium Inoculation with Phosphorus and Nitrogen Fertilizer on Physico - Chemical Properties of the Groundnut Soil. *Environment and Ecosystem Science*, 2(1), 04-06.
- Indan, E., Roslee, R., & Tongkul, F. (2018). Earthquake Vulnerability Assessment (Evas): Analysis of Environmental Vulnerability and Social Vulnerability in Ranau Area, Sabah, Malaysia. *Geological Behavior*, 2(1), 24-28.
- Karami, A., Karamshahi, A., & Shahi, E. (2017). Effects of forestry practices on the regeneration and biodiversity of woody plants in the northern forest ecosystems of Iran. *Geology, Ecology, and Landscape*, 1(4), 264-270.
- Krooss, B. M., Bergen, F. V., & Gensterblum, Y. (2002). High-pressure methane and carbon dioxide adsorption on dry and moisture-equilibrated Pennsylvanian coals. *International Journal of Coal Geology*, 51(2), 69-92.
- Liang, C., Jiang, Z., & Cao, Y. (2016). Deep-water depositional mechanisms and significance for unconventional hydrocarbon exploration: A case study from the lower Silurian Longmaxi shale in the southeastern Sichuan Basin. *AAPG Bulletin*, 100(5), 773-794.
- Liang, X., Ye, X., & Zhang, J. H. (2011). Reservoir forming conditions and favorable exploration zones of shale gas in the Weixin Sag, Dianqianbei Depression. *Petroleum Exploration and Development*, 38(6), 693-699.
- Lu, K., Zhu, X., & Qi, J. (2006). *Petroleum-bearing Basin Analysis*. China University of Petroleum Press, Beijing. pp. 424. (in Chinese).
- M Sarah, M., & Alsier, A. (2018). Protein Digestibility and Amino Acid Content of Malaysian Local Egg Protein Prepared by Different Methods. *Environment and Ecosystem Science*, 2(1), 07-09.
- Nwankwo, C., & Nwankwoala, H. O. (2018). Gully Erosion Susceptibility Mapping in Ikwano Local Government Area of Abia State Using Gis



- Techniques. *Earth Sciences Malaysia*, 2(1), 08-15.
- Nwankwoala, H. O., & Ememu, A. J. (2018). Hydrogeochemical Signatures and Quality Assessment of Groundwater in Okpoko And Environs, Southeastern Nigeria. *Pakistan Journal of Geology*, 2(1), 06-11.
- Nwankwoala, H. O., & Oborie, E. (2018). Geological and Hydrogeological Characterization of a Hydrocarbon Impacted Site in The Niger Delta. *Pakistan Journal of Geology*, 2(1), 12-17.
- Rahim, I. A., Tahir, S., & Musta, B. (2018). Urbanization Vs. Environmental Quality: Some Observation in Telipok, Sabah, Malaysia. *Geological Behavior*, 2(1), 12-17.
- Ross, D. J. K., & Bustin, R. M. (2007). Shale gas potential of the Lower Jurassic Gordondale Member, northeastern British Columbia, Canada. *Bulletin of Canadian Petroleum Geology*, 55, 51–75.
- Ross, D. J. K., & Bustin, R. M. (2009). The importance of shale composition and pore structure upon gas storage potential of shale gas reservoirs. *Marine and Petroleum Geology*, 26, 916–927.
- Su, W., Huff, W. D., & Etensohn, F. R. (2009). K-bentonite, black-shale and flysch successions at the Ordovician–Silurian transition, South China: Possible sedimentary responses to the accretion of Cathaysia to the Yangtze Block and its implications for the evolution of Gondwana. *Gondwana Research*, 15(1), 111–130.
- Sunny, A. A., Omowumi, A., & Chris, O. A. (2018). Improved Magnetic Data Analyses and Enhancement Techniques for Lithological and Structural Mapping Around Akure, Southwestern Nigeria. *Earth Sciences Malaysia*, 2(1), 16-21.
- Zhang, C., Zhang, W., & Guo, Y. (2012). Sedimentary environment and its effect on hydrocarbon source rocks of Longmaxi Formation in Southeast Sichuan and Northern Guizhou. *Earth Science Frontiers*, 19(1), 136–145.
- Zou, C., Dong, D., & Wang, S. (2010). Geological characteristics and resource potential of shale gas in China. *Petroleum Exploration and Development*, 37(6), 641–653.